J. Appl. Comput. Mech., 5(4) (2019) 592-602
DOI: 10.22055/JACM.2018.26947.1364

ISSN: 2383-4536
jacm.scu.ac.ir

M&MoCS

Shahid Chamran University of Ahvaz

Journal of Applied and Computational Mechanics

Research Paper

Transient MHD Convective Flow of Fractional Nanofluid between Vertical Plates

Najma Ahmed[1], Nehad Ali Shah[1,2], BakhtiarAhmad[3], Syed Inayat Ali Shah[3], Sami Ulhaq[3] Mohamad Rahimi-Gorji[4,5]

[1] Abdus Salam School of Mathematical Sciences, GC University Lahore, Pakistan

[2] Department of Mathematics, Lahore Leads University, Lahore Pakistan

[3] Department of Mathematics, Islamia College University Peshawar Khyber Pakhtunkhwa 25000, Pakistan

[4] Experimental Surgery Lab, Department of Surgery, Ghent University, De Pintelaan 185, 9000 Ghent, Belgium

[5] Biofluid, Tissue and Solid Mechanics for Medical Applications Lab (IBiTech, bioMMeda), Ghent University, Gent, Belgium

Received September 01 2018; Revised October 13 2018; Accepted for publication October 15 2018.
Corresponding author: Najma Ahmed, najmaahmed11@gmail.com

Abstract. Effects of the uniform transverse magnetic field on the transient free convective flows of a nanofluid with generalized thermal transport between two vertical parallel plates have been analyzed. The fluid temperature is described by a time-fractional differential equation with Caputo derivatives. Closed form of the temperature field is obtained by using the Laplace transform and fractional derivatives of the Wright's functions. A semi-analytical solution for the velocity field is obtained by using the Laplace transform coupled with the numerical algorithms for the inverse Laplace transform elaborated by Stehfest and Tzou. Effects of the derivative fractional order and physical parameters on the nanofluid flow and heat transfer are graphically investigated.

Keywords: Convection flows; Nanofluids; Caputo fractional derivative; Laplace transform.

1. Introduction

Nanofluids plays an important role in various branches of engineering, for instance industrial cooling systems, nuclear reactors, solar collectors, transportation industries, biochemical applications, heat exchangers, electronic cooling devices and so forth. Therefore, numerous theoretical and computational investigations have been performed on nanofluids in regular surfaces for saving energy as well as getting better performance and minimizing operating costs. However, flow over roughened surface is very common in industries and in several heat transfer devices since irregular surfaces transfer more heat energy compared to flat surfaces. Thus effects of irregular surfaces on convective heat transfer enhancement have been carried out by several investigators.

The concept of a nanofluid has been advanced by Choi [1] who showed substantial augmentation of heat transported in suspensions of copper or aluminum nanoparticles in water and other liquids. Nanofluids are a new kind of fluid; they are dispersions of nanoparticles in liquids that are permanently suspended by Brownian motion. Xuan and Li [2] introduced a procedure for preparing a nanofluid consisting of water and 5 volume% Cu nanoparticles and revealed a great potential of nanofluid in enhancing the thermal conductivity. Khanafer and Vafai [3] analyzed thermo-physical characteristics of nanofluids. They introduced several relative correlations for the thermo-physical properties of nanofluids based on available experimental data. Khanafer et al. [4] investigated the problem of buoyancy-driven heat transfer enhancement of nanofluids in a two-dimensional enclosure. They analyzed four different models based on the physical properties of nanofluid for a range of Grashof numbers and volume fractions. It was found that the suspended nanoparticles substantially increase heat transfer rate

Published online: April 26 2019

for any given Grashof number. Santra et al. [5] conducted a study of heat transfer augmentation in a differently heated square cavity using copper-water nanofluid. Oztop and Abu-Nada [6] studied natural convection flow in nanofluid filled partially heated rectangular enclosures with different types of nanoparticles. Some interesting results exist in literature about natural convection nanofluids are [7-12]. The review of literature clearly indicates that the natural convection flow is mainly related to heated enclosures of regular surfaces filled with nanofluids.

However, none of the above-mentioned papers or books took into consideration fractional derivatives in their governing equations although in the last time the fractional models acquired an increasing interest in many fields including physics, chemistry, biology, heat transfer, quantum mechanics, viscoelasticity, etc. The subject of fractional calculus deals with the investigations of integrals and derivatives of any arbitrary real order. Fractional calculus is now considered as a practical technique in many branches of science including physics (Oldham and Spainier [13]). A growing number of works in science and engineering deal with dynamical system described by fractional order equations that involve derivatives and integrals of non-integer order (Benson et al. [14], Metzler and Klafter [15], Zaslavsky [16]). These new models are more adequate than the previously used integer order models, because fractional order derivatives and integrals describe the memory and hereditary properties of different substances" (Podlubny [17]). This is the most significant advantage of the fractional order models in comparison with integer order models, in which such effects are neglected.

In the recent years, the fluid flow with fractional derivatives become highly emerging area of research. Recently, the effect of fractional order for different fluid have been studied by researchers [18-21], which has been described by fractional partial differential equation and the exact solution of these equations have been obtained by using the discrete Laplace transform, Fourier transform and some well-known special functions.

Up to the author's knowledge, no studies have so far been made with regard to unsteady hydromagnetic free convection of nanofluid flowing between vertical parallel plates with one plate isothermally heated and the other thermally insulated for nanofluids namely copper-water nanofluids with thermal transport described by Caputo time fractional derivatives.

In this work, the fractional differential equation for temperature is solved by using Laplace transform and the partial differential equation for the unsteady fluid flow velocity with appropriate initial and boundary conditions have been solved numerically. The influence of the fractional parameter and physical parameters such as the magnetic interaction parameter, Grashof number, volume fraction on the fluid flow and heat transfer characteristics are analyzed and discussed.

2. Statement of the problem

The transient free convection flow of a nanofluid between two vertical plates separated by a distance L, with one plate isothermally heated and the other one thermally insulated in the presence of a transversal magnetic field of constant intensity B_0 is studied. Initially the temperature of the two plates and of the fluid is assumed to be T_m'. At time $t' > 0$, the plate of $y' = 0$ is kept insulated and the temperature of the plate at $y' = L$ is raised to T_w'. The transient motion of the nanofluid is caused by the buoyancy force arising from the variations of the temperature gradient. The nanofluid is a water-based fluid containing copper/alumina nanoparticles. For the present study, the Prandtl number of water has been considered to be Pr = 6.2 .

The effective density, specific heat capacity, viscosity and thermal conductivity of the nanofluid are given by [18, 22]

$$\rho_{nf} = (1-\phi)\rho_f + \phi\rho_s, \tag{1}$$

$$(\rho c_p)_{nf} = (1-\phi)(\rho c_p)_f + \phi(\rho c_p)_s, \tag{2}$$

$$\mu_{nf} = \frac{\mu_f}{(1-\phi)^{2.5}}, \tag{3}$$

$$\frac{k_{nf}}{k_f} = \frac{k_s + 2k_f - 2\phi(k_f - k_s)}{k_s + 2k_f + \phi(k_f - k_s)}, \tag{4}$$

In the above hypothesis, the governing equations of the considered problem are [22]:

$$\rho_{nf}\frac{\partial u'}{\partial t'} = \mu_{nf}\frac{\partial u'^2}{\partial y'^2} + g(\rho\beta)_{nf}(T' - T_m') - \sigma B_0^2 u', \tag{5}$$

$$(\rho c_p)_{nf}\frac{\partial T'}{\partial t'} = k_{nf}\frac{\partial^2 T'}{\partial y'^2}, \tag{6}$$

where $u'(y',t')$ is the fluid velocity in x-direction, $T'(y',t')$ is the fluid temperature, σ is the electrical conductivity and subscripts f and s refer to the fluid and solid particles, respectively. Along with basic equations (5) and (6) we consider the following initial and boundary conditions:

$$u'(y',0)=0,\ T'(y',0)=T'_m;\quad 0\le y'\le L\,, \tag{7}$$

$$u'(0,t')=0,\ \left.\frac{\partial T'(y',t')}{\partial y'}\right|_{y'=0}=0;\quad t'>0, \tag{8}$$

$$u'(L,t')=0,\ T'(L,t')=T'_w,\ t'>0. \tag{9}$$

Introducing the following dimensionless variables and parameters,

$$y=\frac{y'}{L},\ t=\frac{\nu_f t'}{L^2},\ u=\frac{Lu'}{\nu_f},\ T=\frac{T'-T'_m}{T'_w-T'_m},\ Gr=\frac{g\beta_f L^3(T'_w-T'_m)}{\nu_f^2},\ \mathrm{Pr}=\frac{\mu_f c_{pf}}{k_f},\ M^2=\frac{\sigma B_0^2 L^2}{\mu_f}, \tag{10}$$

into Eqs. (5)-(9), we obtain the dimensionless governing equations, initial and boundary conditions as follow:

$$\frac{\partial u(y,t)}{\partial t}=\frac{1}{(1-\phi)^{2.5}\left[(1-\phi)+\phi\frac{\rho_s}{\rho_f}\right]}\frac{\partial^2 u(y,t)}{\partial y^2}+Gr\left[\frac{(1-\phi)+\phi\frac{(\rho\beta)_s}{(\rho\beta)_f}}{(1-\phi)+\phi\frac{\rho_s}{\rho_f}}\right]T(y,t)-\frac{M^2}{(1-\phi)+\phi\frac{\rho_s}{\rho_f}}u(y,t), \tag{11}$$

$$\frac{\partial T(y,t)}{\partial t}=\frac{k_{nf}}{\mathrm{Pr}\,k_f\left[(1-\phi)+\phi\frac{(\rho c_p)_s}{(\rho c_p)_f}\right]}\frac{\partial^2 T(y,t)}{\partial y^2}, \tag{12}$$

$$u(y,0)=0,\ T(y,0)=0;\ 0\le y\le 1, \tag{13}$$

$$u(0,t)=0,\ \left.\frac{\partial T(y,t)}{\partial y}\right|_{y=0}=0;\quad t>0, \tag{14}$$

$$u(1,t)=0,\ T(1,t)=1;\quad t>0, \tag{15}$$

where Gr is the Grashof number, Pr is the Prandtl number and M^2 is the magnetic parameter. The thermal transport equation (12) has been obtained by using the thermal balance equation and the classical Fourier's law for the thermal flux. In order to consider a mathematical model with thermal memory we followed the ideas from [23, 24]. Generalizing the Fourier's law with Caputo time-fractional derivative, the following fractional mathematical model is studied:

$$\frac{\partial u(y,t)}{\partial t}=\frac{1}{(1-\phi)^{2.5}\left[(1-\phi)+\phi\frac{\rho_s}{\rho_f}\right]}\frac{\partial^2 u(y,t)}{\partial y^2}+Gr\left[\frac{(1-\phi)+\phi\frac{(\rho\beta)_s}{(\rho\beta)_f}}{(1-\phi)+\phi\frac{\rho_s}{\rho_f}}\right]T(y,t)-\frac{M^2}{(1-\phi)+\phi\frac{\rho_s}{\rho_f}}u(y,t), \tag{16}$$

$$D_t^{\alpha}T(y,t)=\frac{k_{nf}}{\mathrm{Pr}\,k_f\left[(1-\phi)+\phi\frac{(\rho c_p)_s}{(\rho c_p)_f}\right]}\frac{\partial^2 T(y,t)}{\partial y^2}, \tag{17}$$

where $D_t^{\alpha}T(y,t)$ is Caputo derivative operator defined as

$$D_t^{\alpha}T(y,t)=\begin{cases}\dfrac{1}{\Gamma(1-\alpha)}\displaystyle\int_0^t\frac{1}{(t-s)^{\alpha}}\frac{\partial T(y,s)}{\partial s}ds; & 0<\alpha<1\\ \dfrac{\partial T(y,t)}{\partial t}; & \alpha=1\end{cases}. \tag{18}$$

3. Solution of the problem

3.1. Temperature distribution

Applying Laplace transform to Eqs. (17), $(14)_2$ and $(15)_2$ and using initial condition Eq. $(13)_2$, we obtain

$$q^{\alpha}\bar{T}(y,q)=\frac{k_{nf}}{\Pr k_f\left[(1-\phi)+\phi\dfrac{(\rho c_p)_s}{(\rho c_p)_f}\right]}\frac{\partial^2\bar{T}(y,q)}{\partial y^2}, \tag{19}$$

$$\left.\frac{\partial\bar{T}(y,q)}{\partial y}\right|_{y=0}=0,\ T(1,q)=\frac{1}{q}. \tag{20}$$

Solution of the partial differential equation (19) subject to conditions in Eq. (20) can be written as

$$\bar{T}(y,q)=\frac{\cosh\left[y\sqrt{a_1}\sqrt{q^{\alpha}}\right]}{q\cosh\left[\sqrt{a_1}\sqrt{q^{\alpha}}\right]} \tag{21}$$

where $a_1=(\Pr k_f b_1)/k_{nf}$, $b_1=(1-\phi)+\phi[(\rho c_p)_s/(\rho c_p)_f]$. In order to obtain the inverse Laplace transform of $\bar{T}(y,t)$ given by Eq. (21), we consider the auxiliary function

$$\begin{aligned}&\bar{F}(y,\mathrm{q})=\frac{1}{q}\frac{\cosh(\mathrm{y}\sqrt{q})}{\cosh(\sqrt{q})}=\frac{1}{q}\frac{e^{y\sqrt{q}}+e^{-y\sqrt{q}}}{e^{\sqrt{q}}+e^{-\sqrt{q}}}=\frac{1}{q}\frac{e^{-(1-y)\sqrt{q}}+e^{-(1+y\sqrt{q})}}{1+e^{-2\sqrt{q}}}=\\&\frac{1}{q}\left[e^{-(1-y)\sqrt{q}}+e^{-(1+y\sqrt{q})}\right]\sum_{k=0}^{\infty}(-1)^k e^{-2k\sqrt{q}}=\sum_{k=0}^{\infty}(-1)^k\left[\frac{e^{-(2k+1-y)\sqrt{q}}}{q}+\frac{e^{-(2k+1+y)\sqrt{q}}}{q}\right],\end{aligned} \tag{22}$$

with the inverse Laplace transform

$$F(y,t)=\sum_{k=0}^{\infty}(-1)^k\left[erfc\left(\frac{2k+1-y}{2\sqrt{t}}\right)+erfc\left(\frac{2k+1+y}{2\sqrt{t}}\right)\right] \tag{23}$$

The Laplace transform (21) can be written in the equivalent form

$$\bar{T}(y,q)=\frac{a_1q^{\alpha}}{q}\frac{\cosh\left[y\sqrt{a_1}\sqrt{q^{\alpha}}\right]}{a_1q^{\alpha}\cosh\left[\sqrt{a_1}\sqrt{q^{\alpha}}\right]}=\frac{a_1}{q^{1-\alpha}}\bar{F}\left(y,a_1q^{\alpha}\right) \tag{24}$$

Using the inverse Laplace transform of the composed functions, we obtain

$$L^{-1}\left\{\bar{F}(y,a_1q^{\alpha})\right\}=\int_0^{\infty}F(y,\mathrm{z})g(z,t)dz \tag{25}$$

where

$$g(\mathrm{z},t)=L^{-1}\left\{e^{-za_1q^{\alpha}}\right\}=\begin{cases}t^{-1}\Phi(0,-\alpha;-a_1\,\mathrm{z}t^{-\alpha}),\ 0<\alpha<1,\\ \delta(t-za_1),\ \alpha=1\end{cases} \tag{26}$$

and

$$t^{\beta-1}\Phi(\beta,-\sigma;-at^{-\sigma})=L^{-1}\left\{\frac{1}{q^{\beta}}e^{-aq^{\sigma}}\right\},\ 0<\sigma<1 \tag{27}$$

In the above relations Φ is the Wright function [25] and $\delta(t)$ is the Dirac's distribution. Now, we have

$$L^{-1}\left\{\bar{F}(y,a_1q^{\alpha}\right\}=\begin{cases}\displaystyle\int_0^{\infty}F(y,z)t^{-1}\Phi(0,-\alpha;-a_1zt^{-\alpha})dz,\ 0<\alpha<1,\\ \dfrac{1}{a_1}F(y,\mathrm{t}/a_1),\ \alpha=1\end{cases} \tag{28}$$

On the other hand, the inverse Laplace of the function $a_1/q^{1-\alpha}$ is

$$L^{-1}\left\{\frac{1}{q^{1-\alpha}}\right\}=\begin{cases}\dfrac{a_1t^{-\alpha}}{\Gamma(1-\alpha)}\quad,0<\alpha<1,\\ a_1\delta(t),\ \alpha=1,\end{cases} \tag{29}$$

Finally, we obtain the temperature field given by

$$T(y,t)=\begin{cases} a_1\int_0^{\infty}F(y,z)\int_0^{t}\frac{(t-\tau)^{-\alpha}}{\Gamma(1-\alpha)}\tau^{-1}\Phi(0,-\alpha;-a_1 z\,\tau^{-\alpha})\,d\tau dz, & 0<\alpha<1,\\ F(y,t/a_1), & \alpha=1. \end{cases} \tag{30}$$

It is easy to look like the relations

$$\begin{aligned} &\Phi(1,-\sigma;-at^{-\sigma})=L^{-1}\left\{\frac{1}{s}e^{-as^{\sigma}}\right\}=\int_0^{t}L^{-1}\left\{e^{-as^{\sigma}}\right\}(\tau)d\tau=\int_0^{t}\tau^{-1}\Phi(0,-\sigma;-\mathrm{a}\,\tau^{-\sigma})d\tau,\\ &\frac{d}{dt}\Phi(1,-\sigma;-at^{-\sigma})=\tau^{-1}\Phi(0,-\sigma;-\mathrm{a}\,\tau^{-\sigma}). \end{aligned} \tag{31}$$

Using Eqs. (30) and (31), we obtain that

$$\int_0^{t}\frac{(t-\tau)^{-\alpha}}{\Gamma(1-\alpha)}\tau^{-1}\Phi(0,-\alpha;-a_1 z\,\tau^{-\alpha})d\tau=\int_0^{t}\frac{(t-\tau)^{-\alpha}}{\Gamma(1-\alpha)}\frac{d}{d\tau}\Phi(1,-\alpha;-a_1 z\,\tau^{-\alpha})d\tau=D_t^{\alpha}\Phi(1,-\alpha;-a_1 z t^{-\alpha}) \tag{32}$$

and, Eq. (30) becomes

$$T(y,t)=\int_0^{\infty}F(y,z)D_t^{\alpha}\Phi(1,-\alpha;-a_1 z t^{-\alpha})\,\mathrm{dz},\ 0<\alpha<1, \tag{33}$$

Therefore, the temperature field is expressed with the Caputo derivative of the Wright's functions.

3.2. Velocity field

Applying the Laplace transform to Eqs. (16), $(14)_1$, $(15)_1$, using the initial condition $(13)_1$ and Eq. (21), we obtain the transformed equation for velocity

$$(b_2 q+b_3)\bar{u}(y,q)=\frac{\partial^2\bar{u}(y,q)}{\partial y^2}+b_4\frac{\cosh\left[y\sqrt{a_1 q^{\alpha}}\right]}{q\cosh\left[\sqrt{a_1 q^{\alpha}}\right]} \tag{34}$$

along with the boundary conditions

$$\bar{u}(0,q)=0,\ \bar{u}(1,q)=0, \tag{35}$$

where

$$b_2=(1-\phi)^{2.5}\left[1-\varphi+\varphi\frac{\rho_s}{\rho_f}\right],\ b_3=M^2(1-\phi)^{2.5},\ b_4=Gr(1-\varphi)^{2.5}\left[(1-\phi)+\phi\frac{(\rho\beta)_s}{(\rho\beta)_f}\right]. \tag{36}$$

The solution of the differential equation (34) along with conditions (35) is given by

$$\bar{u}(y,q)=\bar{u}_1(q)\bar{u}_2(y,q) \tag{37}$$

where

$$\begin{aligned} &\bar{u}_1(q)=\frac{b_4}{(b_2 q+b_3-a_1 q^{\alpha})q\cosh\left(\sqrt{a_1 q^{\alpha}}\right)\sinh\left(\sqrt{b_2 q+b_3}\right)},\\ &\bar{u}_2(y,q)=\cosh\left(\mathrm{y}\sqrt{a_1 q^{\alpha}}\right)\sinh\left(\sqrt{b_2 q+b_3}\right)-\cosh\left(\sqrt{a_1 q^{\alpha}}\right)\sinh\left(y\sqrt{b_2 q+b_3}\right)-\sinh\left((1-\mathrm{y})\sqrt{b_2 q+b_3}\right). \end{aligned} \tag{38}$$

The analytical expression of the Laplace transform $\bar{u}(y,q)$ of velocity $u(y,t)$ being very complicated, we will determine the inverse Laplace transform of velocity using the Stehfest's formula [25], namely

$$u_S(y,t)\approx\frac{\ln(2)}{t}\sum_{j=1}^{2p}d_j\bar{u}\left(y,j\frac{\ln(2)}{t}\right), \tag{39}$$

where

$$d_j = (-1)^{j+p} \sum_{i=\left[\frac{j+1}{2}\right]}^{\min(j,p)} \frac{i^p (2i)!}{(p-i)!\,i!\,(i-1)!\,(j-1)!\,(2i-j)!} \tag{40}$$

where [x] is the integer part of the real number x and p is a positive integer. In order to have a validation of the above results, we used Tzou's [26] algorithm to obtain the inverse Laplace transform of $\bar{u}(y,q)$. Based on Tzou's algorithm [24], the inverse Laplace transform is given by

$$u_T(r,t) = \frac{e^{4.7}}{t}\left[\frac{1}{2}\bar{u}\left(r,\frac{4.7}{t}\right) + \mathrm{Re}\left\{\sum_{k=1}^{N_1}(-1)^k \bar{u}\left(r,\frac{4.7+k\pi i}{t}\right)\right\}\right] \tag{41}$$

where Re(·) is the real part, i is the imaginary unit and N_1 is a natural number.

4. Numerical results and discussions

In order to analyze the influence of the thermal fractional parameter α, nanoparticles volume fraction φ, magnetic parameter M and the Grashof number Gr on the heat transfer and fluid motion, numerical calculations have been carried out and results were presented in graphical illustrations. For the numerical calculations we used the water-copper nanofluid with the following thermo-physical properties [18]:

$$\rho_f = 998.19,\ \rho_s = 8933,\ \beta_f = 21\times10^{-5},\ \beta_s = 1.67\times10^{-5},\ k_f = 0.613,\ k_s = 401,\ (c_p)_f = 4179,\ (c_p)_s = 385 \tag{42}$$

In Fig. 1, the curves corresponding to the fluid temperature $T(y,t)$ at small and large values of the time t, for different values of the fractional parameter α are plotted. From Fig. 1, it is observed that for small values of the time t, the temperature decreases with the fractional parameter; therefore the ordinary fluid has the slowest temperature. For large values of the time t, the temperature increases with the thermal fractional parameter α. This behavior is due to generalized thermal transport in which the temperature gradient-therefore the thermal flux- is damped by the power-law Caputo kernel.

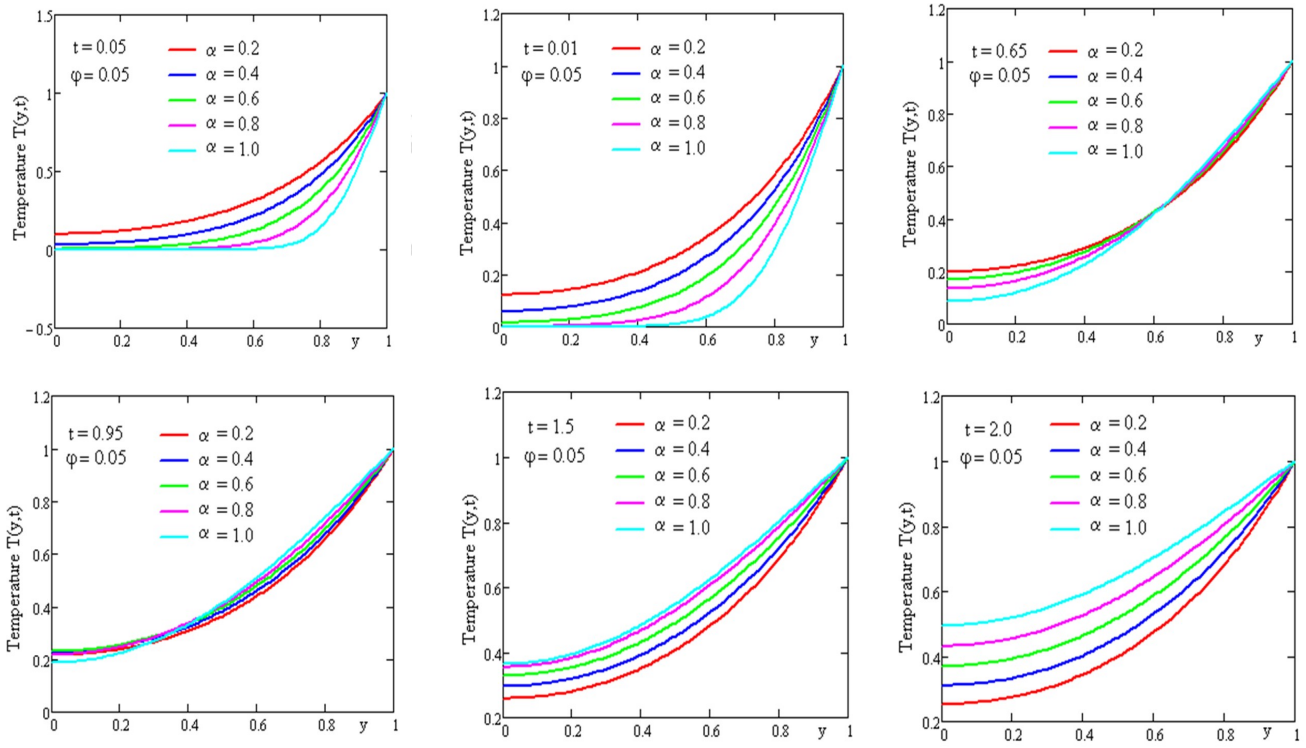

Fig. 1. Profiles of dimensionless temperature versus y for α variation and different values of time t.

The effect of volume fraction φ on the fluid temperature is highlighted by curves in Fig. 2. It is clear that the temperature is increasing function with respect to the nanoparticles volume fraction. It should be noted that the heat transfer process could be improved by the variation of two essential parameters, namely, the fractional coefficient α and the volume fraction φ. Profiles of the fluid velocity at small/large values of the time t and different values of the fractional parameter α have been plotted in Fig. 3 for M = 0.05, Gr = 3 and φ = 0.05. For small values of the time t, the fluid velocity decreases with the fractional parameter. This behavior is in accordance with the temperature variation for small time values. Indeed, at small time values, the temperature decreases with the fractional parameter, therefore the intensity of buoyancy force decreases and fluid flows slower. For large values of the time t the fluid velocity has an opposite behavior as in previous case. The influence of the magnetic parameter M on the fluid motion is presented by curves in Fig. 4.

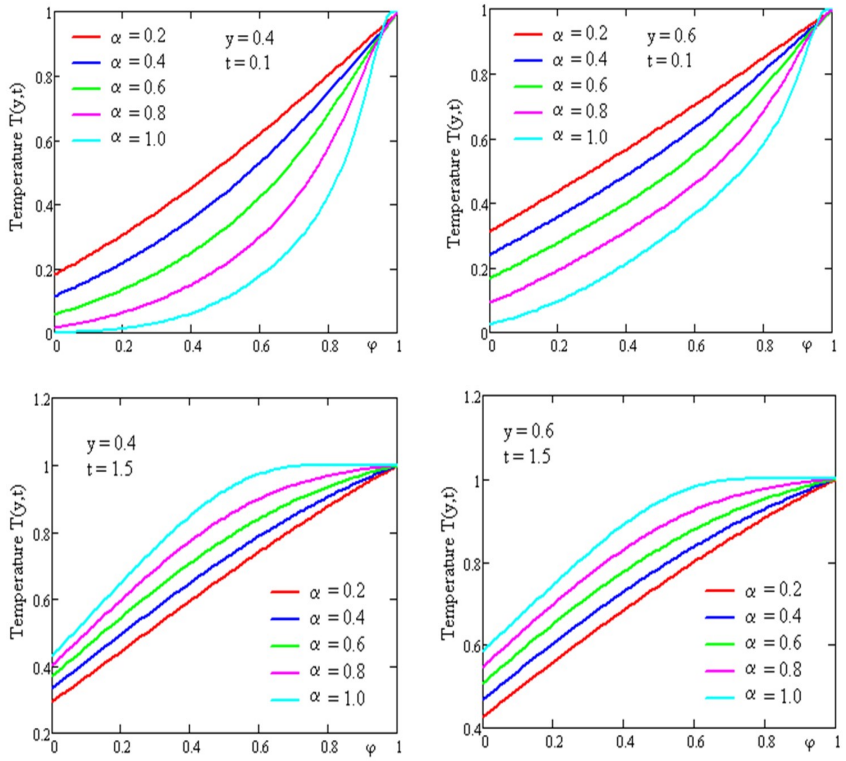

Fig. 2. Profiles of the dimensionless temperature versus volume fraction φ.

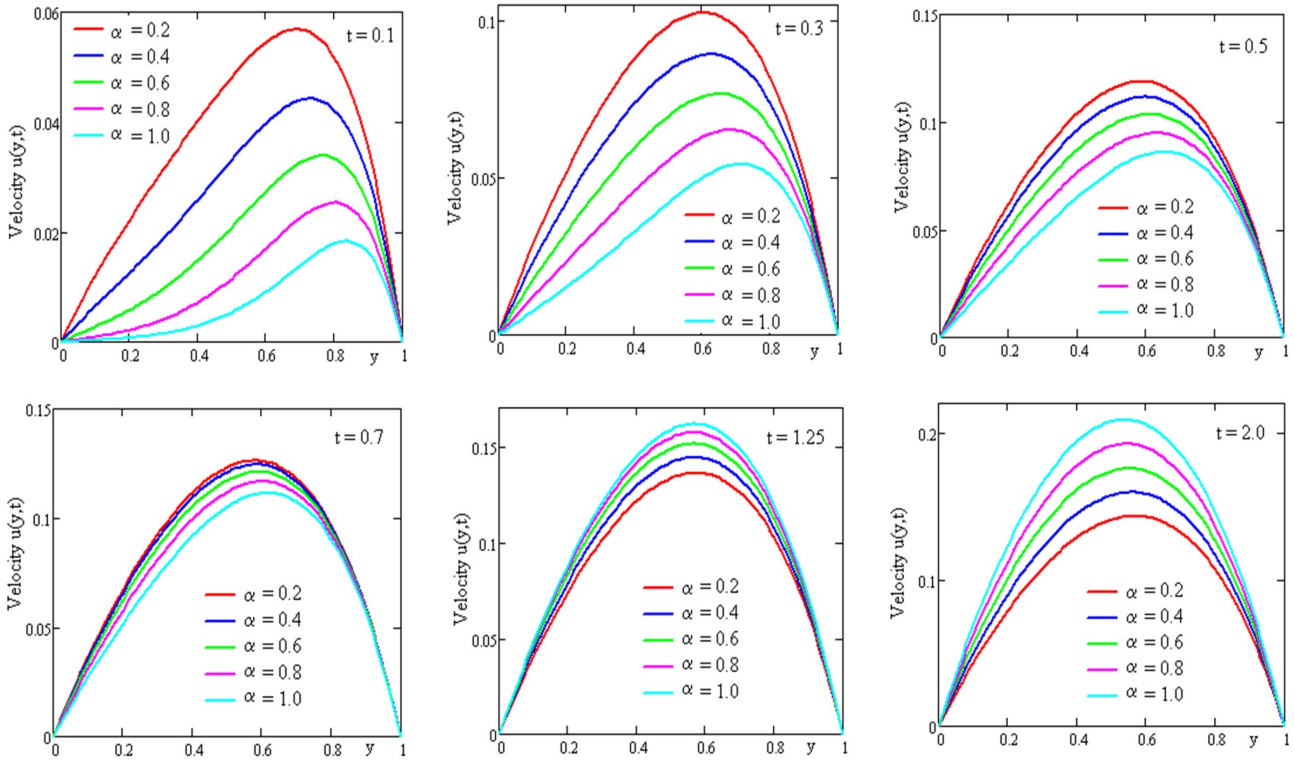

Fig. 3. Profiles of the dimensionless velocity versus y for α variation and different values of time t.

In this figure we have used $Gr = 3$ and $\varphi = 0.05$. As expected the magnetic field acts as a slowing element for fluid movement. The increasing of magnetic field intensity leads to a stronger Lorentz force which is opposite to fluid velocity so, the fluid motion decreases with the magnetic parameter M. Fig. 5 is plotted in order to study effects of the Grashof parameter on the fluid velocity. It is observed from Fig. 5 that the fluid velocity increases with the Grashof number. Indeed, by increasing values of the Grashof number the intensity of buoyancy forces increases and fluid velocity increases. The comparison has between numerical results obtained with Stehfest's and Tzou's algorithms is presented in tables A1-A4 (Appendix A). It can observe that numerical results are in a very good agreement.

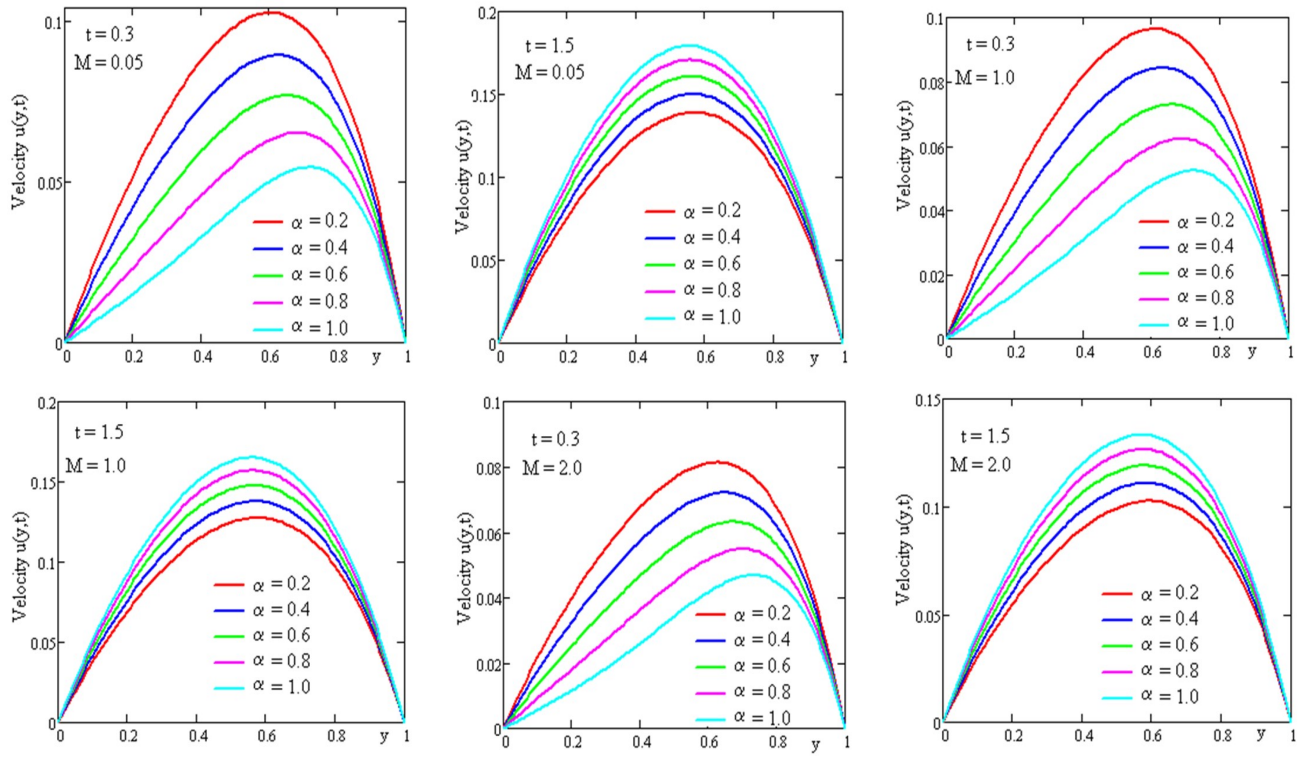

Fig. 4. Profiles of the dimensionless velocity versus y for α variation and different values of the magnetic parameter M.

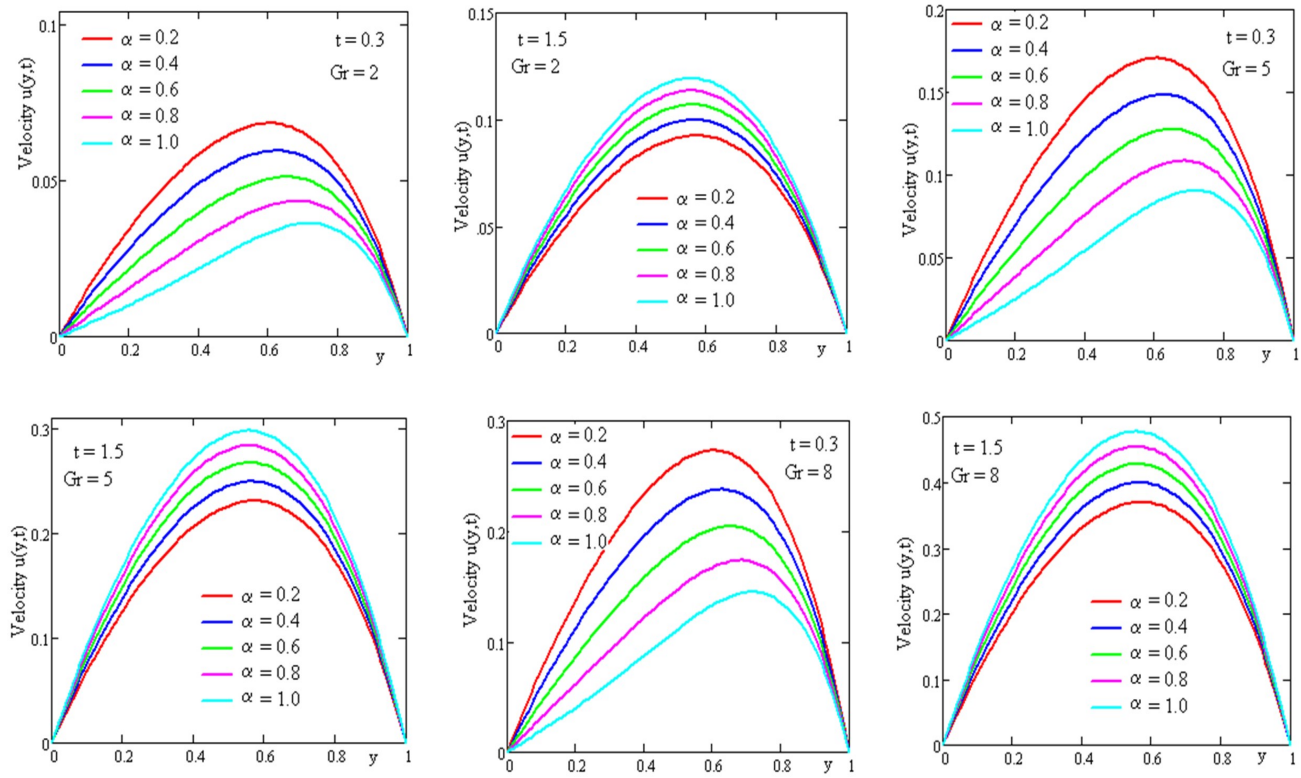

Fig. 5. Profiles of the dimensionless velocity versus y for α variation and different values of the Grashof number Gr.

5. Conclusions

The effects of the thermal fractional parameter α and of the uniform transverse magnetic field on the transient free convective nanofluid flow with fractional thermal transport between vertical asymmetric parallel plates have been analyzed. Closed form of the temperature field and semi-analytical solution of the fluid velocity have been obtained by using the Laplace transform. Numerical inversion techniques of Laplace transform given by Stehfest and Tzou have been employed. To get some physical aspects of the studied problem, we have studied the effects of fractional parameter, volume fraction parameter,

magnetic field and Grashof number on the fluid behavior. The comparison between results given by Stehfest's and Tzou's algorithms is made. The main aims are following:

- For small values of time, increasing the value of fractional parameter the temperature as well as velocity is decreases while the influence is opposite at large value of time.
- The temperature is increase by increasing the number of nanoparticles as well as the time.
- By increasing the magnetic field the velocity is decreases while increasing the Grashof number the velocity is increasing.

Conflict of Interest

The author(s) declared no potential conflicts of interest with respect to the research, authorship and publication of this article.

Funding

The author(s) received no financial support for the research, authorship and publication of this article.

References

[1] Choi, S.U.S., *Enhancing thermal conductivity of fluids with nanoparticles*, in: The proceeding of the 1995 ASME International Mechanical Engineering Congress and Exposition, San Francisco, USA, ASME, FED 231/MD 66 (1995) p. 99-105.
[2] Xuan, Y. and Li, Q., Heat Transfer enhancement of nanofluids, *International Journal of Heat and Fluid Flow*, 21 (2000) 58-64.
[3] Khanafer, K. and Vafai, K., A critical synthesis of thermophysical characteristics of nanofluids, *International Journal of Heat and Mass Transfer*, 54 (2011) 4410-4428.
[4] Khanafer, K., Vafai, K. and Lightstone, M., Buoyancy-driven heat transfer enhancement in a two-dimensional enclosure utilizing nanofluids, *International Journal of Heat and Mass Transfer*, 46 (2003) 3639-3653.
[5] Santra, A.K., Sen, S. and Chakraborty, N., Study of heat transfer augmentation in a differently heated square cavity using copper-water nanofluid, *International Journal of Thermal Sciences*, 47 (2008) 1113-1122.
[6] Oztop, H.F. and Abu-Nada, E., Numerical study of natural convection in partially heated rectangular enclosures filled with nanofluids, *International Journal of Heat and Fluid Flow*, 29 (2008) 1326-1336.
[7] Basak, T. and Chamkha, A.J., Heatline analysis on nanural convection for nanofluids confined within square cavities with various thermal boundary conditions, *International Journal of Heat and Mass Transfer*, 55 (2012) 5526-5543.
[8] Oztop, H.F., Abu-Nada, E., Varol, Y. and Al-Salem, K., Computational analysis of non-isotherm temperature distribution on natural convection in nanofluid filled enclosures, *Superlattices and Microstructures*, 49(4) (2011) 453-467.
[9] Lin, K.C. and Violi, A., Natural convection heat transfer of nanofluid in a vertical cavity: Effects of nonuniform particle diameter and temperature on thermal conductivity, *International Journal of Heat and Fluid Flow*, 31 (2010) 236-245.
[10] Abu-Nada, E., Application of nanofluids for heat transfer enhancement of separated flows encountered in a back ground facing step, *International Journal of Heat and Fluid Flow*, 29 (2008) 242-249.
[11] Wang, X.Q. and Mujumder, A.S., Heat transfer characteristics of nanofluid: a review, *International Journal of Thermal Sciences*, 46 (2007) 1-19.
[12] Eastman, J.A., Choi, S.U.S., Li, S., Thompson, L.J. and Lee, S., *Enhanced thermal conductivity through the development of nanofluids*, in: 1996 Fall meeting of the Materials Research Society (MRS), Boston, USA (1997) p. 3-11.
[13] Oldham, K. B. and Spainier, J., *The Fractional Calculus*, Academic Press, New York, 1974.
[14] Benson, D. A., Wheatcraft, S. W. and Meerschaert, M. M., Application of a fractional advection-dispersion equation, *Water Resources Research*, 36(6) (2000) 1403-1412.
[15] Metzler, R. and Klafter, J., The random walk's guide to anomalous diffusion: A fractional dynamic approach, *Physics Reports*, 339 (2000) 1-77.
[16] Zaslavsky, G. M., Choas Fractional kinetics and anomalous transport, *Physics Reports*, 371(6) (2002) 461-580.
[17] Podlubny, Igor J., *Fractional differential equation*, Academic Press, New York, 1999.
[18] Azhar, W. A., Vieru, D., Fetecau, C., Free convection flow of some fractional nanofluids over a moving vertical plate with uniform heat flux and heat source, *Physics of Fluids*, 29 (2017) 082001.
[19] Imran, M.A., Shah, N.A., Khan, I., Aleem, M., Applications of non-integer Caputo time fractional derivatives to natural convection flow subject to arbitrary velocity and Newtonian heating, *Neural Computing and Applications*, 30(5) (2018) 1589-1599.
[20] Shah, N.A., Khan, I., Heat transfer analysis in a second grade fluid over and oscillating vertical plate using fractional Caputo–Fabrizio derivatives, *European Physical Journal C*, 76 (2016) p. 362.
[21] Imran, M.A., Khan, I., Ahmad, M., Shah, N.A., Nazar, M., Heat and mass transport of differential type fluid with non-integer order time-fractional Caputo derivatives, *Journal of Molecular Liquids*, 229 (2016) 67-75.
[22] Prakash, D., Suriyakumar, P., Transient hydromagnetic convection flow of nanofluid between asymmetric vertical plates with heat generation, *International Journal of Pure and Applied Mathematics*, 113(12) (2017) 1-10.
[23] Ahmed, N., Shah, N. A., Vieru, D., Natural convection with damped thermal flux in a vertical circular cylinder, *Chinese Journal of Physics*, 56 (2018) 630-644.

[24] Hristov, J., *Derivatives with non-singular kernels. From Caputo-Fabrizio definition and beyond*. Frontiers in Fractional Calculus, 1st Edition, Betham Science Publishers, Editor Sachin Bhalekar, p. 269-340, 2017.
[25] Stehfest, H., Algorithm 368: Numerical inversion of Laplace transforms, *Communications of the ACM*, 13 (1970) 47-49.
[26] Tzou, D.Y., *Macro to micro scale heat transfer: The lagging behavior*, Taylor and Francis, Washington, 1997.

Appendix A

Table A1. Comparison of temperature profiles by using Stehfest's and Tzou's algorithm

Y	$\alpha=0.2$ $T_S(y,t)$	$\alpha=0.2$ $T_T(y,t)$	$\alpha=0.2$ $\lvert T_S(y,t)-T_T(y,t)\rvert$	$\alpha=0.8$ $T_S(y,t)$	$\alpha=0.8$ $T_T(y,t)$	$\alpha=0.8$ $\lvert T_S(y,t)-T_T(y,t)\rvert$
0	0.107	0.106	$4.243\text{x}10^{-4}$	$6.108\text{x}10^{-4}$	$6.131\text{x}10^{-4}$	$2.31\text{x}10^{-6}$
0.05	0.108	0.108	$4.373\text{x}10^{-4}$	$7.135\text{x}10^{-4}$	7.159e-4	$2.375\text{x}10^{-6}$
0.1	0.112	0.111	$4.767\text{x}10^{-4}$	$1.049\text{x}10^{-3}$	$1.051\text{x}10^{-3}$	$2.578\text{x}10^{-6}$
0.15	0.118	0.117	$5.443\text{x}10^{-4}$	$1.701\text{x}10^{-3}$	$1.703\text{x}10^{-3}$	$2.939\text{x}10^{-6}$
0.2	0.126	0.126	$6.426\text{x}10^{-4}$	$2.826\text{x}10^{-3}$	$2.83\text{x}10^{-3}$	$3.502\text{x}10^{-6}$
0.25	0.138	0.137	$7.751\text{x}10^{-4}$	$4.679\text{x}10^{-3}$	$4.683\text{x}10^{-3}$	$4.331\text{x}10^{-6}$
0.3	0.152	0.151	$9.465\text{x}10^{-4}$	$7.641\text{x}10^{-3}$	$7.646\text{x}10^{-3}$	$5.506\text{x}10^{-6}$
0.35	0.17	0.169	$1.162\text{x}10^{-3}$	0.012	0.012	$7.101\text{x}10^{-6}$
0.4	0.191	0.19	$1.425\text{x}10^{-3}$	0.019	0.019	$9.154\text{x}10^{-6}$
0.45	0.217	0.215	$1.743\text{x}10^{-3}$	0.03	0.03	$1.166\text{x}10^{-5}$
0.5	0.247	0.244	$2.117\text{x}10^{-3}$	0.046	0.046	$1.458\text{x}10^{-5}$
0.55	0.282	0.279	$2.546\text{x}10^{-3}$	0.068	0.068	$1.791\text{x}10^{-5}$
0.6	0.323	0.32	$3.023\text{x}10^{-3}$	0.099	0.099	$2.177\text{x}10^{-5}$
0.65	0.371	0.368	$3.53\text{x}10^{-3}$	0.142	0.142	$2.634\text{x}10^{-5}$
0.7	0.427	0.423	$4.032\text{x}10^{-3}$	0.2	0.2	$3.181\text{x}10^{-5}$
0.75	0.492	0.487	$4.467\text{x}10^{-3}$	0.276	0.276	$3.824\text{x}10^{-5}$
0.8	0.566	0.562	$4.732\text{x}10^{-3}$	0.372	0.372	$4.548\text{x}10^{-5}$
0.85	0.653	0.648	$4.664\text{x}10^{-3}$	0.492	0.492	$5.01\text{x}10^{-5}$
0.9	0.753	0.748	$4.015\text{x}10^{-3}$	0.636	0.636	$1.928\text{x}10^{-4}$
0.95	0.868	0.865	$2.404\text{x}10^{-3}$	0.806	0.804	$2.348\text{x}10^{-3}$

Table A2. Comparison of temperature profiles by using Stehfest's and Tzou's algorithm

ϕ	$t=0.5$ $T_S(y,t)$	$t=0.5$ $T_T(y,t)$	$t=0.5$ $\lvert T_S(y,t)-T_T(y,t)\rvert$	$t=1.5$ $T_S(y,t)$	$t=1.5$ $T_T(y,t)$	$t=1.5$ $\lvert T_S(y,t)-T_T(y,t)\rvert$
0.01	0.034942	0.034955	$1.264\text{x}10^{-5}$	0.448349	0.448407	$5.806\text{x}10^{-5}$
0.02	0.037451	0.037464	$1.313\text{x}10^{-5}$	0.457173	0.457231	$5.865\text{x}10^{-5}$
0.03	0.040053	0.040067	$1.361\text{x}10^{-5}$	0.465986	0.466045	$5.918\text{x}10^{-5}$
0.04	0.042749	0.042763	$1.409\text{x}10^{-5}$	0.474789	0.474849	$5.966\text{x}10^{-5}$
0.05	0.045538	0.045553	$1.458\text{x}10^{-5}$	0.483582	0.483642	$6.016\text{x}10^{-5}$
0.06	0.04842	0.048436	$1.506\text{x}10^{-5}$	0.492365	0.492425	$6.055\text{x}10^{-5}$
0.07	0.051395	0.051411	$1.554\text{x}10^{-5}$	0.501138	0.501199	$6.092\text{x}10^{-5}$
0.08	0.054462	0.054478	$1.602\text{x}10^{-5}$	0.5099	0.509961	$6.13\text{x}10^{-5}$
0.09	0.05762	0.057637	$1.65\text{x}10^{-5}$	0.518651	0.518713	$6.163\text{x}10^{-5}$
0.1	0.06087	0.060887	$1.698\text{x}10^{-5}$	0.527391	0.527453	$6.199\text{x}10^{-5}$
0.11	0.06421	0.064227	$1.746\text{x}10^{-5}$	0.536118	0.53618	$6.231\text{x}10^{-5}$
0.12	0.06764	0.067658	$1.794\text{x}10^{-5}$	0.544832	0.544894	$6.266\text{x}10^{-5}$
0.13	0.071161	0.071179	$1.843\text{x}10^{-5}$	0.55353	0.553594	$6.306\text{x}10^{-5}$
0.14	0.07477	0.074789	$1.891\text{x}10^{-5}$	0.562213	0.562277	$6.349\text{x}10^{-5}$
0.15	0.078468	0.078488	$1.94\text{x}10^{-5}$	0.570878	0.570942	$6.402\text{x}10^{-5}$
0.16	0.082255	0.082275	$1.989\text{x}10^{-5}$	0.579523	0.579588	$6.464\text{x}10^{-5}$
0.17	0.08129	0.08615	$2.039\text{x}10^{-5}$	0.588148	0.588213	$6.542\text{x}10^{-5}$
0.18	0.090092	0.090113	$2.089\text{x}10^{-5}$	0.596749	0.596815	$6.631\text{x}10^{-5}$
0.19	0.094141	0.094163	$2.14\text{x}10^{-5}$	0.605325	0.605392	$6.737\text{x}10^{-5}$
0.2	0.098278	0.0983	$2.191\text{x}10^{-5}$	0.613874	0.613942	$6.869\text{x}10^{-5}$

Table A3. Comparison of velocity profiles by using Stehfest's and Tzou's algorithm

Y	$\alpha=0.2$ $u_S(y,t)$	$\alpha=0.2$ $u_T(y,t)$	$\alpha=0.2$ $\lvert u_S(y,t)-u_T(y,t)\rvert$	$\alpha=0.8$ $u_S(y,t)$	$\alpha=0.8$ $u_T(y,t)$	$\alpha=0.8$ $\lvert u_S(y,t)-u_T(y,t)\rvert$
0	0	0	0	0	0	0
0.05	0.027688	0.027686	$1.948\text{x}10^{-6}$	0.018779	0.018784	$5.613\text{x}10^{-6}$
0.1	0.053584	0.053586	$2.15\text{x}10^{-6}$	0.036815	0.036826	$1.088\text{x}10^{-5}$
0.15	0.077671	0.077676	$5.547\text{x}10^{-6}$	0.054128	0.054143	$1.566\text{x}10^{-5}$
0.2	0.0999	0.099906	$6.191\text{x}10^{-6}$	0.070694	0.070714	$1.965\text{x}10^{-5}$
0.25	0.120186	0.12019	$4.433\text{x}10^{-6}$	0.086448	0.08647	$2.242\text{x}10^{-5}$
0.3	0.13841	0.138411	$1.603\text{x}10^{-6}$	0.101272	0.101296	$2.339\text{x}10^{-5}$

Table A3. Continued

Y	$\alpha = 0.2$ $u_S(y,t)$	$\alpha = 0.2$ $u_T(y,t)$	$\alpha = 0.2$ $\lvert u_S(y,t) - u_T(y,t)\rvert$	$\alpha = 0.8$ $u_S(y,t)$	$\alpha = 0.8$ $u_T(y,t)$	$\alpha = 0.8$ $\lvert u_S(y,t) - u_T(y,t)\rvert$
0.35	0.154414	0.154414	$4.981\text{x}10^{-7}$	0.115003	0.115025	$2.2\text{x}10^{-5}$
0.4	0.168002	0.168002	$2.304\text{x}10^{-8}$	0.127418	0.127436	$1.794\text{x}10^{-5}$
0.45	0.178936	0.178941	$4.648\text{x}10^{-6}$	0.138237	0.138249	$1.15\text{x}10^{-5}$
0.5	0.186932	0.186945	$1.375\text{x}10^{-5}$	0.147116	0.14712	$4.012\text{x}10^{-6}$
0.55	0.191657	0.191683	$2.575\text{x}10^{-5}$	0.15364	0.153638	$1.867\text{x}10^{-6}$
0.6	0.192728	0.192764	$3.619\text{x}10^{-5}$	0.157321	0.157319	$2.249\text{x}10^{-6}$
0.65	0.189703	0.18974	$3.734\text{x}10^{-5}$	0.157594	0.157601	$6.857\text{x}10^{-6}$
0.7	0.182075	0.182094	$1.888\text{x}10^{-5}$	0.153815	0.153842	$2.71\text{x}10^{-5}$
0.75	0.169263	0.169233	$2.969\text{x}10^{-5}$	0.145266	0.14532	$5.474\text{x}10^{-5}$
0.8	0.150597	0.150482	$1.155\text{x}10^{-4}$	0.13115	0.131229	$7.888\text{x}10^{-5}$
0.85	0.125303	0.125067	$2.36\text{x}10^{-4}$	0.110595	0.110674	$7.936\text{x}10^{-5}$
0.9	0.092479	0.092124	$3.55\text{x}10^{-4}$	0.082634	0.082656	$2.251\text{x}10^{-5}$
0.95	0.05109	0.050751	$3.397\text{x}10^{-4}$	0.046173	0.046091	$8.193\text{x}10^{-5}$

Table A4. Comparison of velocity profiles by using Stehfest's and Tzou's algorithm

ϕ	$t = 0.5$ $u_S(y,t)$	$t = 0.5$ $u_T(y,t)$	$t = 0.5$ $\lvert u_S(y,t) - u_T(y,t)\rvert$	$t = 1.5$ $u_S(y,t)$	$t = 1.5$ $u_T(y,t)$	$t = 1.5$ $\lvert u_S(y,t) - u_T(y,t)\rvert$
0.01	0.148746	0.148756	$9.726\text{x}10^{-6}$	0.282172	0.282199	$9.726\text{x}10^{-6}$
0.02	0.148519	0.148527	$8.257\text{x}10^{-6}$	0.279331	0.279362	$8.257\text{x}10^{-6}$
0.03	0.148169	0.148176	$6.807\text{x}10^{-6}$	0.276356	0.27639	$6.807\text{x}10^{-6}$
0.04	0.1477	0.147706	$5.388\text{x}10^{-6}$	0.273254	0.273292	$5.388\text{x}10^{-6}$
0.05	0.147116	0.14712	$4.012\text{x}10^{-6}$	0.27003	0.270072	$4.012\text{x}10^{-6}$
0.06	0.146421	0.146423	$2.691\text{x}10^{-6}$	0.26669	0.266736	$2.691\text{x}10^{-6}$
0.07	0.145617	0.145618	$1.436\text{x}10^{-6}$	0.263241	0.26329	$1.436\text{x}10^{-6}$
0.08	0.144709	0.14471	$2.592\text{x}10^{-7}$	0.259687	0.259741	$2.592\text{x}10^{-6}$
0.09	0.143702	0.143701	$8.298\text{x}10^{-7}$	0.256035	0.256093	$8.298\text{x}10^{-7}$
0.1	0.142598	0.142596	$1.821\text{x}10^{-6}$	0.252289	0.252351	$1.821\text{x}10^{-6}$
0.11	0.141401	0.141399	$2.705\text{x}10^{-6}$	0.248455	0.248521	$2.705\text{x}10^{-6}$
0.12	0.140117	0.140113	$3.475\text{x}10^{-6}$	0.244538	0.244609	$3.475\text{x}10^{-6}$
0.13	0.138748	0.138743	$4.123\text{x}10^{-6}$	0.240543	0.240619	$4.123\text{x}10^{-6}$
0.14	0.137298	0.137293	$4.644\text{x}10^{-6}$	0.236476	0.236556	$4.644\text{x}10^{-6}$
0.15	0.135772	0.135767	$5.033\text{x}10^{-6}$	0.232341	0.232426	$5.033\text{x}10^{-6}$
0.16	0.134173	0.134168	$5.286\text{x}10^{-6}$	0.228143	0.228233	$5.286\text{x}10^{-6}$
0.17	0.132506	0.1325	$5.403\text{x}10^{-6}$	0.223887	0.223982	$5.403\text{x}10^{-6}$
0.18	0.130773	0.130767	$5.381\text{x}10^{-6}$	0.219578	0.219679	$5.381\text{x}10^{-6}$
0.19	0.128979	0.128973	$5.223\text{x}10^{-6}$	0.215221	0.215327	$5.223\text{x}10^{-6}$
0.2	0.127126	0.127121	$4.93\text{x}10^{-6}$	0.21082	0.210931	$4.93\text{x}10^{-6}$